Cite this paper as:

Georgopoulos, A., & Agrafiotis, P. (2012, September). Documentation of a submerged monument using improved two media techniques. In Virtual Systems and Multimedia (VSMM), 2012 18th International Conference on (pp. 173-180). IEEE.

Documentation of a submerged monument using improved two media techniques

A. Georgopoulos, P. Agrafiotis
Laboratory of Photogrammetry
School of Rural & Surveying Eng., NTUA
Athens Greece
drag@central.ntua.gr

Abstract— The rapid developments of technology in recent years have opened new horizons in Photogrammetry, overcoming obstacles sometimes insurmountable, reducing time and increasing accuracy of results. However, while the continuous development of close-range Photogrammetric methods for the geometric documentation of monuments on land and sea seem to go hand in hand, techniques for capturing submerged archaeological sites especially when situated at shallow depths are inadequate while application of traditional methods is impossible or uneconomical. This paper describes the improvement of two-media (through air and water) photogrammetric techniques for the documentation of a submerged archaeological site of Epidaurus, Greece, at a depth ranging from 0.5 to 2 meters. Specific reference is made to the various problems caused by the presence of water and how they were addressed. Errors in depth determination caused by waves, colour absorption and chromatic aberration are also addressed. Particular attention is given to the effects of refraction at the air/water interface on the Collinearity Condition. The various attempts are presented, analysed and evaluated. Finally, ortho-images have been generated and cross section data were collected in order to perform the documentation.

Keywords: two media photogrammetry, refraction, camera calibration, orthophotography

I. INTRODUCTION

It is common knowledge that the sea level is rising. Consequently, but also due to other geological phenomena, structures situated at the shoreline are gradually submerged to various depths under the sea surface. Especially in the Mediterranean area, with the undeniable wealth of monuments this situation is becoming very critical. Cultural Heritage on the other hand should be documented, preserved and inherited to future generations. Hence, the geometric documentation of submerged monuments becomes extremely critical.

For this purpose, two approaches are usually employed. Firstly, transferring all documentation activity, i.e. measurements, image acquisition etc., completely underwater and, secondly performing all data acquisition from outside, in case of shallow waters.

A. Documentation underwater

Underwater methods are usually based on pure surveying techniques, such as distance measurements and trilateration for network adjustments (Diamanti et al. 2011; Barkai & Kahanov, 2007; Benjamin & Bonsall, 2009) or even on more sophisticated methods, such as use of sound waves for positioning (e.g. Thomson and Elson, 2002; Holt, 2004; 3H Consulting, 2009). The use of photogrammetric methods for data acquisition offers, contrary to the above, high accuracy, the ability to measure more details, less contact with the object and the construction of 3D textured models. During the recent years it seems that there is an increasing number of such applications (e.g. Diamanti et al. 2011; Canciani et al., 2003; Pizarro et al., 2004; Singh et al., 2005; Abdo et al., 2006; Drap et al., 2007; Shortis et al., 2007a,b). In these cases the camera is used in a special underwater housing device for obvious protection.

For the processing of these image data, two different approaches are reported. One is based on the geometric interpretation for light propagation through various media (e.g. air – housing device – water) and the other on the application of suitable corrections, in order to compensate for the refraction. Some researchers use a pinhole camera for the estimation of the refraction parameters (π.χ. Van der Zwaan et al., 2002; Pizarro et al., 2004; Singh et al., 2005), while others calibrate the cameras with the help of an object of known dimensions, which is put underwater in situ (Gracias and Santos-Victor, 2000; Pessel et al., 2003; Höhle, 1971). Self calibration is also applied for the camera-housing system, where it is assumed that refraction effects are compensated by the interior orientation parameters (Shortis and Harvey ,1998; Gründig et al., 1999; Canciani et al., 2003; Harvey et al.,2003; Drap et al., 2007; Shortis et al., 2007b). However, when analyzing the correction of the image points, especially for close ranges, the distance of the object points from the camera severely affects the correction (Telem and Filin, 2010). Hence it is concluded that a simple correction of the image points is not adequate.

B. Two media documentation

In case of two media applications the camera is above the water surface and the object submerged (Butler et al, 2002). Two media photogrammetric techniques have been extensively reported (e.g. Tewinkel, 1963; Shmutter and Bonfiglioli, 1967; Mastry, 1974; Karara, 1972; Slama, 1980; Shan, 1994) and the basic optical principles prove that photogrammetric processing through water is possible. However, in the literature no case of monument geometric recording has been reported so far.

Two media photogrammetric techniques have been used for mapping underwater areas using some kind of special platform for hoisting the camera (Whittlesey, 1975; Fryer, 1983a; Westaway et al., 2001). These applications have adopted some way for correcting the refraction effect at the water surface. Aerial images have also been used for mapping the sea bottom with an accuracy of approximately 10% of the water depth in cases of clear waters and shallow depths, i.e. 5-10m (Byrne and Honey, 1978; Harris and Umbach, 1972; Masry, 1975).

For mapping an underwater area, Elfick and Fryer (1983) used a "floating pyramid" for lifting the two cameras. The base of the pyramid was made of Plexiglas for avoiding wave effects and sun glint (1983a). For correcting the refraction effect while performing the stereorestitution, Snell's law was applied knowing the incident angles of the rays and the camera constant.

A more contemporary application is reported by Butler et al. (2002) for mapping the bottom of a river. The extracted DTM points have been corrected from refraction effects, base on a specially developed algorithm. A Plexiglas surface was again used for carrying the control points.

For modelling a scale-model rubble-mound breakwaters (Ferreira et al., 2006), refraction effects were described via a linearized Taylor series, which is valid for paraxial rays. In this way a virtual principal point has been defined where all rays were converging. It has been shown that this approach offers satisfactory compensations for the two media involved.

Usually a plane surface is assumed in photogrammetric procedures through water, so that the distance of the submerged object from that surface is constant, while the taking distance is varying from image to image. (Shmutter and Bonfiglioli, 1967; Ke et al., 2008). In some cases the water-air surface is modeled by an harmonic wave (Okamoto, 1982).

It should be noted finally, that in cases of automation, i.e. stereomatching algorithms, there is an increased uncertainty level for obvious reasons.

II. Task Description

A. Description of the site

The area of Epidaurus is known from the era of Homer. It has been a key place, mainly because of its geographic position and its important ancient harbor (Papahatzis, 1976). Apart from the well known antiquities on dry land, there are a lot of ancient constructions in the sea near or far from today's shoreline. They were buildings at the sea front, which have been submerged due to the elevation of the sea surface. There have been several attempts for their documentation (Kritzas 1972) using aerial photography from a tethered balloon and from a height of 150m. One such building was spotted approximately 50 m from the shore and is imaged in Figure 1.

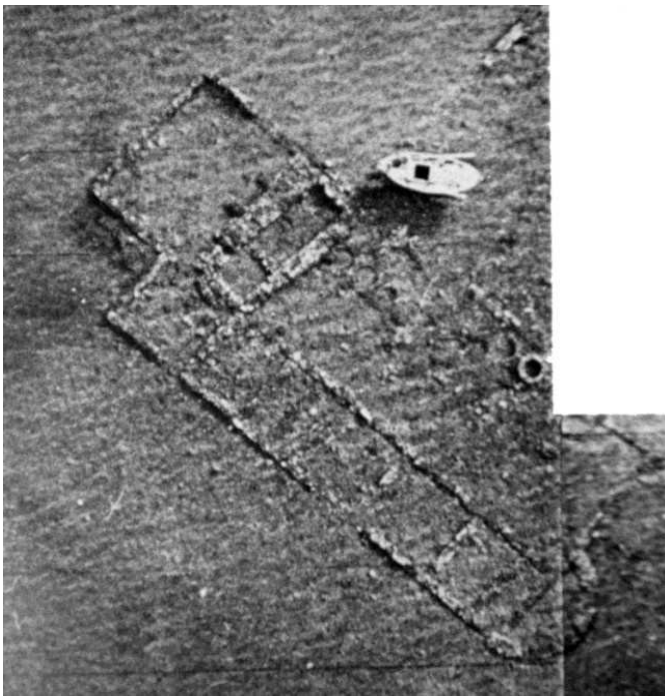

Figure 1: The archaeological site photographed from a balloon (Kritzas, 1972)

It is this particular building that was documented implementing the methodology developed and described in this paper. It is situated at a depth ranging from 0.5 to 3m and its dimensions are 50x45m.

B. Fieldwork

Data acquisition was carefully planned, in order to ensure the best conditions both for surveying measurements and taking the images. Firstly a 3 point network was established ashore in order to enable control point measurements. The adjustment of this network was performed with an accuracy of 5mm.

Images were taken with a Canon EOS MIII full frame DSLR with a resolution of 21Mpixel. A 16mm super wide angle lens was used, as it was expected that due to the refraction effects the imaged area would actually be smaller than under normal conditions. The camera was hoisted approximately 6 m above the water surface with the help of a specially developed tripod (Figure 2).

A day with practically no wind was chosen for the photography. Care was taken in order to ensure a constant overlap of 80% and maintain a straight "flight".

Figure 2: Image acquisition with the tripod

GCP's were later spotted on the images and they were measured from the network points using a total station and a prism. Due to the unavoidable currents, the pointing accuracy was deteriorating resulting to a mean uncertainty of 30mm. These points were later used for the photogrammetric processing (Figure 3).

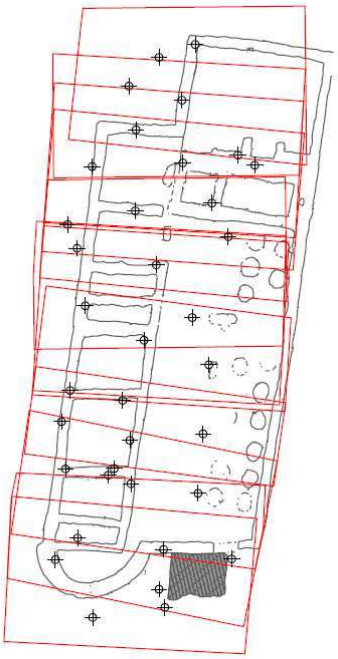

Figure 3: Distribution of GCP's and the layout of the overlaps

C. *Defining the problems*

The data acquisition conditions, briefly described above caused a number of problems. Refraction on the water surface was a major, but expected, cause of distortion. The not even water surface caused geometric distortions, which could not be modeled. Moreover sun glint was unavoidable. Even though the time of photography was close to midday, reflections on the small waves made parts of the images useless. In addition, the fact that light went twice through the water surface, caused chromatic aberrations, different for the various angles of incidence.

III. METHODOLOGY APPLIED

A. *Camera Calibration*

Initially it was thought that a suitable camera calibration would compensate for all distortions caused by optical anomalies, like refraction, radial distortion, etc. Hence, camera calibration was performed in air and in two media using the camera calibration software provided by Photomodeler® software by EOS.

Figure 4a,b,c: Raw calibration images in air(a) and two media (b) and camera positions(c).

The results of the second calibration were not as expected. In cases of in-water calibration and due to the larger refractive index, the effective camera constant is by a factor of 1.34 larger than the one in plain air. As this was not the case, it was decided to use the plain air interior orientation parameters.

Media	Camera constant c (mm)	xp (mm)	yp (mm)	RMS xy (pixel)	RMS XYZ (mm)	# images
air	16.519	17.901	12.045	0.212	0.061	9
air - water	15.483	17.743	11.683	6.262	2.310	7

Table 1:Camera Calibration results in air and air-water

The large differences appearing in Table 1 are due to certain problems which are caused by the presence of the two media. Refraction is causing an apparent lifting of the imaged objects lying at depths as small as 0.50m. As a result the test field used for the calibration is imaged at a different scale and the template matching techniques used by Photomodeler do not succeed. It seems that in the case of two media photography, the 1.34 factor does not apply. It has been established (Agrafiotis & Georgopoulos 2012) that in such cases the most probable relation of the effective camera constant to the one in air is given by

$$P_{air} * 1 + P_{water} * 1.33 \quad (1)$$

P_{air} and P_{water} are the percentages of air and water respectively that intervene between camera and object.

B. *Radiometric Corrections*

The initial images are of very low radiometric quality, because of the adverse light absorption since the object is submerged. Hence, suitable radiometric corrections were applied in order to enhance them and enable the photogrammetric measurements.

The most important processing action was the HDR toning, which was applied to the images. In this way the processed image is assigned the features of a High Dynamic Range

image, without multiple exposures with the bracketing sequence. This is replaced by “edge glow”, “tone and detail”, “color”, and “toning curve and histogram” actions (Figure 5).

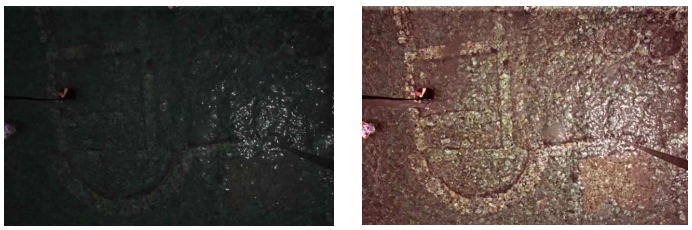

Figure 5: Initial image (left) and processed (left) with HDR toning

C. *Effect of ripples*

The effect of the ripples on the water surface is quite intense in the images (Figure 6). It is obvious that they will influence the photogrammetric adjustments. Because of the time delay between two consecutive images, the water surface is differentiating and the distortions caused by the ripples are unique in each image.

According to Fryer and Kniest (1985) the errors caused by the ripples to depth calculation are due to two main reasons: the width of the wave and the non verticality of the local normal. Besides as the waves move, the actual height of the water above a point is changing and this affects the refraction of its image (Fryer and Kniest, 1985). According to Masry and MacRitchie (1980), the most important component (75%) of the total error in determining depth, is the deviation of the normal from the local vertical. Those errors do not follow the normal distribution. Considering the conditions of the image acquisition in the present case, an error of 60mm is expected at a mean depth of 0.85m.

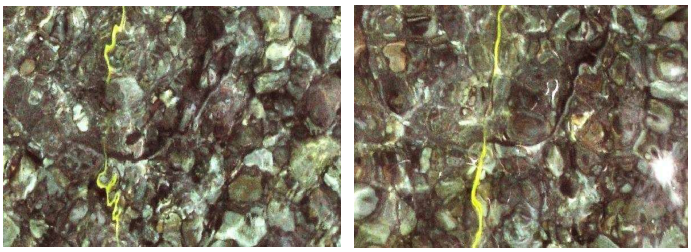

Figure 6: Imaging of a linear object (yellow line) deformed by the ripples

D. *Refraction*

Refraction is the most probable cause of geometric distortions in the case of two media photography. As already stated, the refraction effect could not be corrected by a suitable camera calibration. Hence it was decided to develop an algorithm which would free the images from this adverse effect. This correction would be applied before any photogrammetric procedure, including the interior orientation, in order to use the parameters calculated for one medium, i.e. air.

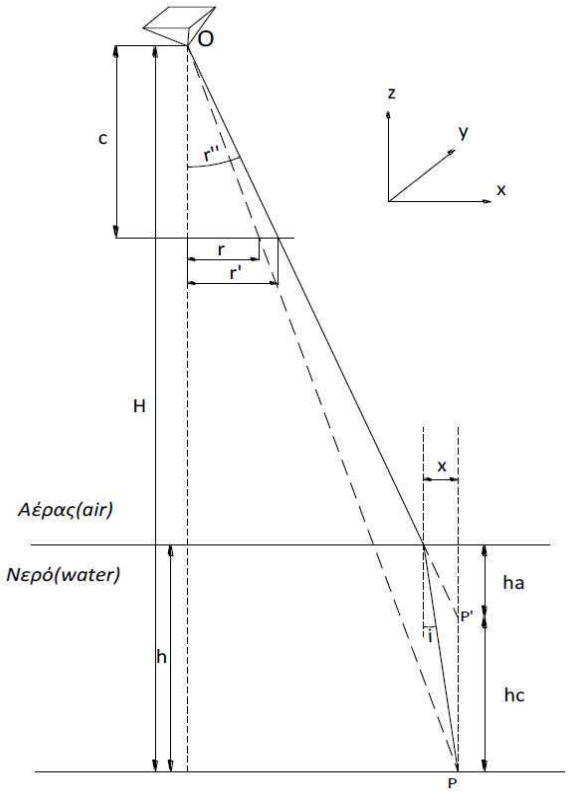

Figure 7: The geometry for two media photogrammetry

For the development of the software, the surface of the water was considered to be planar and horizontal. Moreover it was assumed that from a point P on the object a ray is emitted, which after refraction hits a pixel of the image at a distance r' from its center.

According to *Snell’s law* :

$$i = \sin^{-1}\left(\frac{\sin r''}{n}\right) \qquad (2)$$

where i=incident angle, r''=refraction angle and n=refractive index. From Figure 7:

$$\begin{aligned} h_A &= x / \tan r'' \\ h_A &= x / \tan i \end{aligned} \qquad (3)$$

where x is the positional error between the exit point of the ray and the real position of the point.

Hence:

$$h = \frac{h_A \tan r''}{\tan i} \qquad (4)$$

From equations (2) and (4) we get (Butler et al., 2002) :

$$h = \frac{h_A \tan r''}{\tan\left(\sin^{-1}\left(\frac{\sin r''}{n}\right)\right)} \qquad (5)$$

Which, for all realistic values of r" may be approached from the following:

$$h = \frac{h_A \tan r''}{\tan\left(\frac{r''}{n}\right)} \qquad (6)$$

From Figure 7 we may get :

$$r'' = a\tan\left(\frac{r'}{c}\right)$$
$$h_c = h - h_a \qquad (7)$$

The equations (7) are the ones used for developing the algorithm, which will correct the images from refraction. As input it accepts the depth for all imaged points, the camera height and the refractive index *n*. Additionally, the camera constant in pixels and the principal point coordinates (dx_o, dy_o in pixel) are also necessary.

The algorithm works as follows:

The radial distance r' of each pixel is calculated from the principal point. Afterwards the depth h is read from the relevant table and with the help of equations 7 the new corrected radial distance is determined. A new image is gradually constructed using the determined radial distances and the colour value which corresponds to the pixel corrected. It should be noted that for r'=0 refraction correction was considered zero. The result of the algorithm is a new image of the same dimensions and resolution as the initial one. On this image the object seems to occupy smaller area, which is due to the refraction geometry (Figure 8).

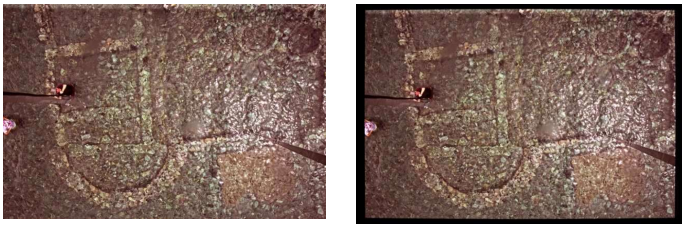

Figure 8:Raw Image (left) and corrected from refraction (right)

For entering the depth values of all pixels, a routine of the algorithm extracts the corresponding depth value from a depth image. This latter contains raster depth information, with variation of grey values and depicts areas of mean depth value for every 50mm (Figure 9).

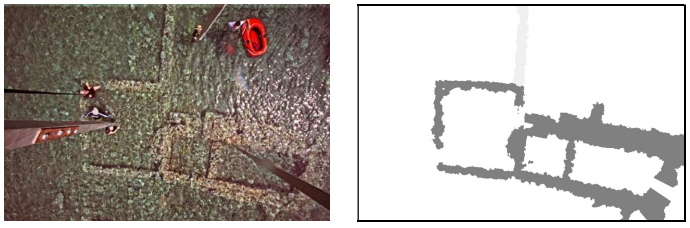

Figure 9:Initial non corrected image (left) and raster depth map of the same area (right)

The maximum uncertainty was calculated, caused by the maximum possible error (50mm) both in XY and in Z: $\sigma_{x,y}$=±0,008m and σ_z=±0,030m.

E. Adjustments

The acquired images were adjusted in a strip with block adjustment using the Image Master® software by Topcon. Two such adjustments were performed, one with the uncorrected images and one with the corrected ones. In both cases relative and absolute orientation results were compared and for the case of the corrected image block, a Digital Surface Model (DSM) was produced and from that an orthophoto.

IV. EXPERIMENTAL RESULTS

A. Relative orientation

92 tie points were used in total. Those of them that presented the maximum y-parallax errors are situated in stereopairs in which the water depth imaged is large or their distribution is not favourable.

Stereo pair	Residual y-parallax (pixel)		Tie points	
	Corr	NC	Corr	NC
1	0.74	0.59	8	8
2	0.70	0.11	6	6
3	0.45	0.98	6	6
4	0.65	0.79	7	7
5	0.45	0.67	6	6
6	0.17	0.97	7	7
7	0.87	0.84	7	7
8	0.88	0.34	6	7
9	0.88	0.84	7	6
10	0.42	0.80	7	7
11	0.78	0.96	7	7
Mean	0,64	0,72		

Table 2: Residual y-parallax after the relative orientation

In Table 2 it is worth noticing that no significant differences are observed between the two blocks (Corrected and Non corrected, NC). Hence they are not representative for the problems caused by refraction to the shape of the object.

B. Absolute Orientation

For the absolute orientation, 13 of the GCP's were used in each block, the same for both. The rest were used as control points. Pointing of the points in the non corrected block was more difficult the in the corrected one.

GCP	DX (m)		DY (m)		DZ (m)	
	Corr	NC	Corr	NC	Corr	NC
1	0.032	0.0004	0.036	0.047	0.019	0.098
2	-0.046	-0.010	-0.003	-0.019	-0.043	-0.071
3	-0.022	-0.033	0.009	0.009	-0.038	-0.053
4	0.040	0.026	0.136	0.135	0.008	0.0296
5	0.124	0.111	0.120	0.088	-0.049	-0.060
6	-0.104	-0.062	-0.153	-0.185	0.094	0.001
7	-0.054	0.001	0.057	-0.088	0.075	0.075
8	0.001	-0.063	-0.025	0.042	0.124	0.076
9	-0.060	-0.075	0.033	0.020	-0.064	-0.103
10	0.0462	0.078	-0.078	-0.111	0.025	0.027
11	0.0917	0.080	0.043	0.058	-0.056	-0.025
12	-0.0014	-0.040	-0.014	-0.013	0.012	0.062
13	0.154	0.133	-0.024	0.042	-0.042	-0.031
Mean	**0.075**	**0.068**	**0.074**	**0.083**	**0.059**	**0.062**

Table 3: Errors in the GCP's after Absolute Orientation

It is obvious that the differences between the two adjustments are not significant. What is significant is that the errors in the case of the corrected image block are more uniform in X, Y and Z. It should be noted that while pointing on the GCP's, the errors in the case of the non corrected block remained large. The software drove the user to very wrong pointings in order to correct the results. This may be explained by the erroneous formation of the shape at the stage of the relative orientation.

It is worth mentioning that for the assessment of the refraction effects the direction of the residual errors is a very important parameter in addition, of course, to their magnitude. Figure 10 (left) shows that all GCP's residuals in a non corrected stereomodel had a systematic outward radial trend profoundly due to the refraction effect. In contrast, it is obvious that in a corrected stereomodel (Figure 10 right) this systematic effect is eliminated, leaving only the displacements due to the ripples.

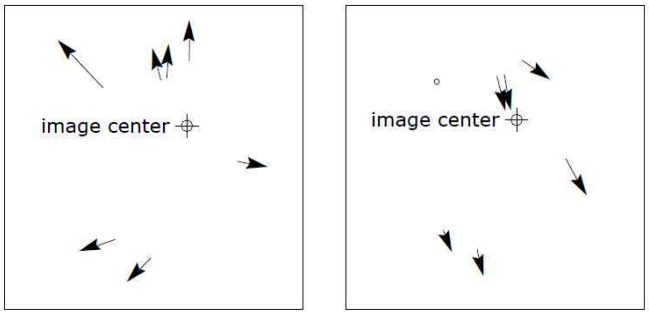

Figure 10: GCP's residuals in a non corrected (left) and a corrected (right) stereomodel

C. DSM and Orthophotography

The main problem in DSM acquisition was the deformations of the object at the water surface, mainly due to the ripples. Sun glint was also a severe cause of errors. As a result it was often impossible for the software to correctly match conjugate points in adjacent images. Consequently, the DSM for the whole block was extracted using a combination of a manual and an automatic methodology.

In Figure 11 an example of a DSM of a planar object produced exclusively automatically is shown.

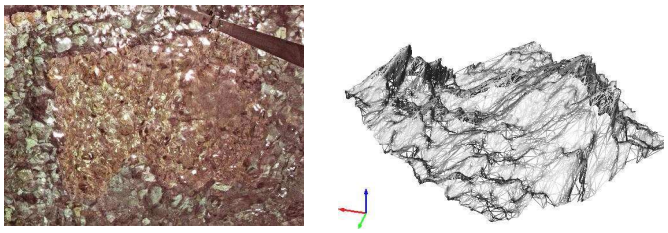

Figure 11: The automatically collected DSM of a planar object

It should be noted that the peaks have common orientation, which is identical with the direction of the waves. In most cases of objects at the edge of the overlaps there were insurmountable problems. Due to that, it was decided to manually enter the necessary break lines and collect DSM only from the central part of the images. For the whole area approximately 27 DSM's were collected which were combined later to form the global DSM of the area.

The inevitable problems in the DSM have caused deformations in the resulting orthophotos (Figure 12). The effects were deformed areas, geometric distortions and also radiometric deformations, which were successfully solved by correcting the DSM.

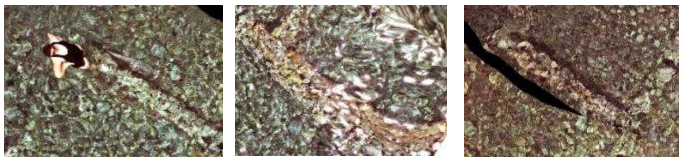

Figure 12: Occlusions of image information by human recklessness (left), sun glint (middle)and non existen information

The final orthophoto was produced separately for the walls and the bottom. For the latter a rather sparse DSM, i.e. 10cm resolution, was collected. The resulting orthophoto is depicted in Figure 13.

The accuracy levels achieved are adequate for a geometric documentation at a scale of 1:200. This is a common scale for general drawings for archaeological purposes. If greater accuracy is required, i.e. for larger scales, larger image scales should be employed, which would inevitably result in greater number of images.

Figure 13: The combined orthophoto

V. CONCLUDING REMARKS

Two media techniques are very useful for documenting submerged monuments at shallow waters. However, special care should be taken in order to compensate for all adverse effects caused by refraction, sun glint, ripples etc. In this report it has been shown that with the development of a simple algorithm the effect of the refraction may be removed from two media images, in order to perform the photogrammetric procedures. On the other hand high accuracy is difficult to achieve in those cases and special care should be taken in order to keep the errors to a minimum.

REFERENCES

[1] 3H Consulting, 2009. *Techniques: acoustic positioning systems*. http://www.3hconsulting.com/TechniquesAcoustics.htm

[2] Abdo, D.A., Seager, J.W., Harvey, E.S., McDonald, J.I., Kendrick, G.A., Shortis, M.R., 2006. *Efficiently measuring complex sessile epibenthic organisms using a novel photogrammetric technique*. Journal of Experimental Marine Biology and Ecology 339 (1), 120-133.

[3] Agrafiotis P., Georgopoulos, A., 2012. *Evaluation and Comparison of Digital Camera Calibration Methods*. 4th National Metrology Conference, Athens February 2012 (in Greek).

[4] Barkai, O., Kahanov, Y., 2007. *The Tantura F shipwreck, Israel*. International Journal of Nautical Archaeology, 36(1), 21-31.

[5] Benjamin, J., Bonsall, C., 2009. *A feasibility study for the investigation of submerged sites along the coast of Slovenia*. International Journal of Nautical Archaeology, 38 (1), 163-172.

[6] Butler, J.B., Lane, S.N., Chandler, J.H., Porfiri, E., 2002. *Through-Water Close Range Digital Photogrammetry In Flume and Field Environment*. Photogrammetric Record. 17(99) Q 419-439.

[7] Byrne, P.M. and Honey, F.R., 1978. *Air Survey and Satellite Imagery Tools for Shallow Water Bathymetry*. Inst. Of Surveyors Aust. Congress, Darwin, pp. 103-119.

[8] Canciani, M., Gambogi, P., Romano, F.G., Cannata, G., Drap, P., 2003. Low cost digital photogrammetry for underwater archaeological site survey and artifact insertion. The case study of Dolia wreck in secche della meloria-livorno-italia. International Archives of the Photogrammetry, Remote Sensing and Spatial Information Sciences 34 (Part5/W12), 95-100.

[9] Diamanti, E., Georgopoulos, A., Vlachaki, F., 2011. *Geometric documentation of underwater archaeological sites.* XIII CIPA International Symposium, Prague 2011.

[10] Drap, P., Seinturier, J., Scaradozzi, D., Gambogi, P., Long, L., Gauch, F., 2007. *Photogrammetry for virtual exploration of underwater archeological sites.* In: Proc. XXIth CIPA International Symposium, Athens, Greece, 1-6 October.

[11] Elfick, M.H. and Fryer, J.G., 1983. *Mapping in Shallow Water*. University of Newcastle, Australia, Commission V, pp. 240-247.

[12] Ferreira, R., Costeira, J.P., Silvestre, C., Sousa, I. and Santos, J.A., 2006. *Using Stereo Image Reconstruction to Servey Scale Models of Rubble-Mound Structures*. First International Conference on the Application of Physical Modelling to Port and Coastal Protection.

[13] Fryer, J.G., 1983. *Photogrammetry through shallow water*. Australian Journal of Geodesy, Photogrammetry and Surveying, 38: 25-38.

[14] Fryer, J.G., 1983b. *A Simple System for Photogrammetric Mapping in Shallow Water*. Photogrammetric Record, 11(62), pp. 203-208.

[15] Fryer, J.G., 1984. Errors in depths determined by through-water photogrammetry. Ibid., 40: 29-39.

[16] Fryer, J.G. and Kniest, H.K., 1985. Some strategies for improving the accuracy of depths determined by through-water photogrammetry. Ibid, 43: 45-60.

[17] Fryer, J.G. and Kniest, H.K., 1985. *Errors in Depth Determination Caused by Waves in Through-Water Photogrammetry*. Photogrammetric Record, 11(66): 745-753.

[18] Gracias, N., Santos-Victor, J., 2000. *Underwater video mosaics as visual navigation maps.* Computer Vision and Image Understanding 79 (1), 66-91.

[19] Gründig, L., Moncrieff, E., Schewe, H., 1999. The CoSMoLUP project for the improvement of fishfarm pen design using computational structural modelling and large-scale underwater photogrammetry. In: Astudillo, R., Madrid, A. J. (Eds.), Proc. IASS 40th Anniversary Congress, 20-24 September, Madrid, Spain, IASS/CEDEX

[20] Harris, W.D. and Umbach, M.J., 1972. *Underwater Mapping*. Photo. Eng., 38(6), pp. 765-772.

[21] Harvey, E.S., Cappo, M., Shortis, M.R., Robson, S., Buchanan, J., Speare, P., 2003. The accuracy and precision of underwater measurements of length and maximum body depth of southern bluefin tuna (Thunnus maccoyii) with a stereo-video camera system. Fisheries Research 63 (3), 315-326.

[22] Höhle, J., 1971. *Reconstruction of the underwater object*. Photogrammetric Engineering 37 (9), 949_954.

[23] Holt, P., 2004. *The application of the fusion positioning system to marine archaeology*. In: Congress on the Application of Recent Advances in Underwater Detection and Survey Techniques to Underwater Archaeology.

[24] Karara, H.M., 1972. *Simple cameras for close-range applications*. Photogrammetric Engineering, 38(5): 447-451.

[25] Ke, X., Sutton, M.A., Lessner, S.M., Yost, M., 2008. Robust stereo vision and calibration methodology for accurate three-dimentional digital image correlation measurements on submerged objects. The Journal of Strain Analysis for Engineering Design 43(8), 689-704.

[26] Kritzas, Ch., V., 1972. News from the city of Epidaurus. Athens Archaeological Annals, V,2, pp. 186-199 (in Greek).

[27] Masry, S.E., 1975. *Measurement of Water Depth by Analytical Plotter*. International Hydrographic Review, 52, 1, pp. 75-86.

[28] Masry, S. E. and MacRitchie, S., 1980. *Different considerations in coastal mapping*. Phofogrammetric Engineering and Remote Sensing, 46(4): 521-528.

[29] Okamoto, A., 1982. *Wave influences in two-media photogrammetry*. Photogrammetric engineering and Remote Sensing, 48(9): 1487-1499.

[30] Okamoto, A., 1984. Orientation problem of two-media photographs with curved boundary surfaces. Ibid., 50(3): 303-316.

[31] Papachatzis, N., 1976. Pausanias' *Periegesis, Corinthos-Lacony,* Athens.

[32] Pessel, N., Opderbecke, J., Aldon, M.J., 2003. *Camera self-calibration in underwater environment*. In: Proc. The 11-th International Conference in Central Europe on Computer Graphics, Visualization and Computer Vision, Plzen - Bory, Czech Republic, 3-7 February, pp. 104-110.

[33] Pizarro, O., Eustice, R., Singh, H., 2004. *Large area 3d reconstructions from underwater surveys*. In: Proc. IEEE/MTS OCEANS Conference and Exhibition, 2, Kobe, Japan, 9-12 November, pp. 678-687.

[34] Shan, J., 1994. *Relative orientation for two-media photogrammetry*. Photogrammetric Record, 14(84): 993-999.

[35] Shmutter, B, and Bonfiglioli, L, 1967. *Orientation problems in two-medium photogrammetry*. Photogrammetric Engineering, 33(12): 1421-1428.

[36] Shortis, M.R., Harvey, E.S., 1998. *Design and calibration of an underwater stereovideo system for the monitoring of marine fauna populations.* International Archives Photogrammetry and Remote Sensing 32 (5), 792-799.

[37] Shortis, M.R., Harvey, E.S., Seager, J.W., 2007a. *A review of the status and trends in underwater videometric measurement.* In: SPIE Conference 6491, Videometrics IX, IS&T/SPIE Electronic Imaging, San Jose, CA, USA.

[38] Shortis, M.R., Seager, J.W., Williams, A., Barker, B.A., Sherlock, M., 2007b. *A towed body stereo-video system for deep water benthic habitat surveys.* In: Grün, A., Kahmen, H. (Eds.), Proc. Eighth Conference on Optical 3-D Measurement Techniques, ETH Zurich, Switzerland, 2, pp. 150-157.

[39] Slama, C.C. (Editor-in-Chief), 1980. *Manual of Photogrammetry*, Fourth edition, American Society of Photogrammetry, Falls Church, Virginia, 1056 pages.

[40] Singh, H., Roman, C., Pizarro, O., Eustice, R., 2005. *Advances in high resolution imaging from underwater vehicles.* In: Proc. 12th International Symposium of Robotics Research, October 2005, pp. 430-448.

[41] Telem, G., Filin, S., 2010. *Photogrammetric modeling of underwater environments*. ISPRSJournal of Photogrammetry and Remote Sensing.

[42] Tewinkel, G.C., 1963. *Water depths from aerial photographs*. Photogrammetric Engineering, 29(6): 1037-1042.

[43] Thomson, D., Elson, S., 2002. *New generation acoustic positioning systems*. In: Proc. OCEANS'02 MTS/IEEE, 3, pp. 1312-1318.

[44] Van der Zwaan, S., Bernardino, A., Santos-Victor, J., 2002. *Visual station keeping for floating robots in unstructured environments*. Robotics and Autonomous Systems 39 (3-4), 145-155.

[45] Westaway, R.M., Lane, S.N. and Hicks, D.M., 2001. *Remote sensing of clear-water, shallow, gravel-bed rivers using digital photogrammetry*. Photogrammetric Engineering & Remote Sensing, 67(11): 1271-1281.

[46] Whittlesey, J., 1975. *Elevated and Airbone Photogrammetry and Stereo Photography, in Photography an Archaelogical Research*. edited by Elmer Harp JNR., Univ. of New Mexico Press, Albuquerque, pp.223-258.